A&A manuscript no.
(will be inserted by hand later)

Your thesaurus codes are:
02.04.01, 08.14.1, 08.16.6, 02.07.01

ASTRONOMY
AND
ASTROPHYSICS
1.2.2008

Rapid differential rotation of protoneutron stars and constraints on radio pulsars periods

J-O. Goussard[2], P. Haensel[1,2], and J.L. Zdunik[1]

[1] N. Copernicus Astronomical Center, Polish Academy of Sciences, Bartycka 18, PL-00-716 Warszawa, Poland
[2] Département d'Astrophysique Relativiste et de Cosmologie, UPR 176 du CNRS, Observatoire de Paris, Section de Meudon, F-92195 Meudon Cedex, France
e-mail : goussard@obspm.fr, haensel@camk.edu.pl, jlz@camk.edu.pl

Abstract. Models of differentially rotating protoneutron stars are calculated, using realistic equations of state of dense hot matter. Various conditions within the stellar interior, corresponding to different stages of protoneutron star evolution, are considered. Numerical calculations are performed within the approximation of stationary equilibrium, using general relativistic equations of stationary motion of differentially rotating, axially symmetric stars and using a numerical code based on spectral methods. Families of differentially rotating models of a given baryon mass are calculated, using a two-parameter formula describing the angular velocity profile within a rotating protoneutron star. Apart from the usual "mass shedding limit", we introduce an additional "minimal mass limit" for differentially rotating protoneutron stars resulting from a type II supernovae. Maximum angular momentum, which can be accommodated by a protoneutron star within these limits is calculated, for various thermal conditions in stellar interior, for a baryon mass of 1.5 $M_\odot$. In the case of a thermally homogeneous (isentropic or isothermal) neutrino-opaque interior this maximum angular momentum turns out to be somewhat higher than that of a cold neutron star of the same baryon mass, rotating uniformly at the mass shedding angular velocity. However, if the protoneutron star has a thermal structure characteristic of initial state, with a low entropy (unshocked) core, and a high entropy (shocked) outer half of baryon mass, the maximum angular momentum is significantly lower. This leads to a minimum period of uniform rotation of cold neutron stars of baryon mass ~ 1.5 $M_\odot$, formed directly (i.e. without a subsequent significant accretion of mass) from protoneutron stars with shocked envelope, of about 1.7 ms and strengthens the hypothesis that millisecond pulsars are accretion accelerated neutron stars.

Key words: dense matter – stars: neutron – stars: pulsars

Send offprint requests to: J-O. Goussard

1. Introduction

Newly born neutron stars are expected to be quite different from ordinary neutron stars, which are a commonly accepted model of radio pulsars. Just after their formation in a gravitational collapse of a massive stellar core, a future neutron star is a hot (internal temperature $\sim 10^{11}$ K), lepton rich (one electron for three nucleons) object - in view of these specific features it is called a *protoneutron star*. After some seconds, a protoneutron star transforms into a neutron star, loosing the lepton number excess via emission of neutrinos trapped in dense, hot stellar interior. The short period of neutrino burst is of paramount importance for the fate of collapsing star. It is commonly accepted, on the basis of numerical simulations of gravitational collapse of stellar cores, that the prompt-shock mechanism fails to make a successful explosion corresponding to a SN II. It is currently believed, that neutrino flow from a protoneutron star can revive the stalled shock. It is thus clear that the structure and evolution of a protoneutron star, formed as a product of gravitational collapse, are crucial for the success (or failure) of the accretion shock revival, and therefore, for a successful SN II explosion.

While the lifetime of a protoneutron star (seconds) is negligibly short compared with the lifetime of a neutron star at the radio pulsar stage, it is some three orders of magnitude longer than the dynamical timescale for these objects (milliseconds). In view of this one can study the bulk evolution of protoneutron stars in the quasistationary approximation, treating convection just as an additional transport process in the stellar interior. Static properties of protoneutron stars, under various assumptions concerning their composition and equation of state of hot, dense interior, were studied by numerous authors (Burrows & Lattimer 1986, Takatsuka 1995, Bombaci et al. 1995, Bombaci 1996, Prakash et al. 1997, Gondek et al. 1997).

The formation of a protoneutron star (PNS) occurs on a dynamical timescale. It involves compression, with an overshoot of central density, and a hydrodynamical bounce. PNS is expected to begin its life pulsating around its quasistatic equilibrium. Radial pulsations of PNS were recently studied in (Gondek et al. 1997).

If the presupernova core was rotating - even very slowly, the PNS is expected to be rather rapidly rotating. This is an inevitable consequence of the conservation of the angular momentum of the collapsing core, which during a fraction of a second shrinks to about one percent of its initial radius. The effects of rotation on the process of collapse of massive stellar core were studied in Mönchmeyer & Müller (1989), Janka & Mönchmeyer (1989) and Yamada & Sato (1994).

Rapid rotation can have a strong effect on the structure of a PNS. The effect of rotation is stronger than in the case of cold neutron stars (NS), because a hot PNS, due to the thermal and neutrino trapping effects, is a more extended object than a cold configuration of the same baryon (rest) mass. Rapid uniform rotation of PNS was studied recently in (Hashimoto et al. 1995, Goussard et al. 1997), who considered also the consequences of the rotational properties of PNS for cold NS, into which a PNS transforms due to deleptonization and cooling.

Uniform rotation of PNS should be considered as a first step in the study of their rotational properties. Even if the presupernova core was uniformly rotating, collapse would generate a significant amount of differential rotation of PNS (during collapse, each collapsing annulus conserves – to a very good approximation – its angular momentum with respect to the rotation axis). Numerical simulations of collapse of rotating stellar cores indicate a characteristic distribution of angular velocity within a newly formed PNS : angular velocity of the matter, which is approximatively constant on coaxial cylinders, decreases with increasing distance from the rotation axis (Mönchmeyer & Müller 1989, Janka & Mönchmeyer 1989).

Evolutionary timescales of a PNS are at most seconds; actually, the lifetime of a PNS is shorter than about twenty seconds (the time needed for the hot stellar interior to deleptonize). The only mechanisms which we could contemplate as the means of a sufficiently rapid transport of angular moment on such a short timescale are related to the superstrong magnetic fields, convection and, maybe, turbulent viscosity. Our knowledge of the quantitative role of these effects, which could rigidify rotation of PNS, is at present insufficient to make reliable estimate of rigidification timescale. On the other hand, the viscous timescale, related to the transport of neutrinos within the hot, neutrino opaque interior of a PNS, is much longer than the PNS lifetime.

In the present paper we generalize our previous calculations of the models of rapidly rotating PNS (Goussard et al. 1997) to the case of differential rotation. In particular, we study to what extent the presence of differential rotation modifies the conclusions obtained assuming uniform rotation of PNS, referring to the limitations imposed on the periods of solitary pulsars formed directly from PNS. Existing calculations of rapid differential rotation were restricted to the case of *cold* NS (Wilson 1972, Komatsu et al. 1989), and used schematic (unrealistic) equations of state of $T = 0$ neutron star matter. Our models of hot, differentially rotating PNS are constructed using a realistic EOS of dense hot matter, taking into account both the effects of high temperature, and of trapped neutrinos.

The model of the dense, hot interior of PNS is described in Sect. 2. We begin with a short description of the assumed thermal and lepton structure. Then we present the equation of state of the PNS matter, corresponding to various stages of the PNS evolution. We discuss also characteristic timescales, relevant for PNS, and justify the assumption of stationarity (hydrostatic equilibrium) of rotating PNS. The mathematical formulation of the problem of stationary differential rotation of PNS is presented in Sect. 3, where we also consider the problem of stability of differentially rotating PNS. The numerical method of solution of equations of stationary motion is described in Sect. 4, where we also discuss in some detail the problem of precision of our numerical solutions. In Sect. 5 we present our models of rapidly, differentially rotating PNS, and discuss in particular the mass shedding limits for these models, at various stages of PNS evolution. We study also the relation between differentially rotating PNS and uniformly rotating cold NS. Finally, Sect. 6 contains the discussion of our results and our conclusions.

2. Physical conditions in the interior of a protoneutron star

Our models of PNS are based on available results of (mostly 1-D) simulations of neutron star birth (Burrows & Lattimer 1986, Janka & Mönchmeyer 1989, Mönchmeyer & Müller 1989, Burrows et al. 1995). We consider PNS just after it settled into a quasi-stationary state (we neglect pulsations which could be excited due to hydrodynamical overshoot and bounce). As we restrict ourselves to the period after the successful revival of the standing (accretion) shock, we can neglect the effects of accretion. In what follows, we will consider three situations. The first one corresponds to a very initial state of a PNS, which is then composed of a hot shocked envelope, with entropy per baryon (in the units of $k_{\rm B}$) $s_{\rm env} \sim 5-10$ up to some baryonic density $n_{\rm env}$, and an unshocked core, characterized by $s_{\rm core} \sim 1$ above some density $n_{\rm core} > n_{\rm env}$. The layer with $n_{\rm env} < n < n_{\rm core}$ constitutes a transition region between the unshocked core and the shocked envelope. Our standard model of a PNS will have baryon (rest) mass of $M_{\rm bar} = 1.5\ {\rm M}_\odot$. Then, the shocked envelope will contain about $0.7\ {\rm M}_\odot$ of the baryon mass. Both core and envelope are neutrino opaque - a neutrino transparent outer layer of the envelope has a negligible mass, and was not

included. We will hereafter call such a protoneutron star configuration an early-type PNS (EPNS).

The second situation (established after 0.2-0.5 s, see Burrows & Lattimer 1986, Keil et al. 1996) will correspond to a thermally homogeneous PNS. At this stage, the thermal state of PNS interior (below the neutrinosphere) is characterized by $s \sim 2$, and some characteristic lepton fraction Y_l. This situation will be referred to as a late-type PNS (LPNS).

Further cooling and deleptonization transforms PNS into a NS of the same $M_{\rm bar}$. The structure of a sufficiently cool NS (internal temperature $T < 10^{10}$ K) is determined essentially by the $T = 0$ EOS; due to strong degeneracy thermal effects in the EOS of the dense NS interior can be completely neglected. This will correspond to a third situation considered by us. The three situations, described in this paragraph, correspond to quite different EOS of the stellar interior, described below.

2.1. Equations of state and stationary models of PNS

We will assume a well defined "neutrinosphere" which separates a hot, neutrino-opaque interior from colder neutrino–transparent envelope. Hot dense matter in the hot, neutrino opaque interior is composed of nucleons (both free and bound in nuclei) and leptons (electrons, positrons, and neutrinos and antineutrinos of all flavors; for simplicity we do not include muons). Nucleon component of hot matter will be described by one of the models developed by Lattimer & Swesty (1991), corresponding to the incompressibility of symmetric nuclear matter at saturation density $K = 220$ MeV. The local state of matter in the hot interior is determined by the baryon (nucleon) number density n, the net electron fraction $Y_e = (n_{e^-} - n_{e^+})/n$, and the net fraction of trapped electron-neutrinos, $Y_\nu = (n_{\nu_e} - n_{\bar{\nu}_e})/n$. An initial stage of PNS evolution is characterized by a significant trapped lepton number $Y_l = Y_\nu + Y_e \simeq 0.4$. Under these conditions, both electrons and electron–neutrinos are strongly degenerate. The deleptonization, due to the ν_e diffusion outward (driven by the gradient of the chemical potential of ν_e) and subsequent emission from their neutrinosphere, implies a strong decrease of Y_l on a timescale of seconds (Sawyer & Soni 1979, Prakash et al. 1997). After the deleptonization (which for simplicity is assumed to be complete, with $Y_\nu = 0$), there is no trapped lepton number, so that neutrinos trapped within the hot interior do not influence the beta equilibrium of nucleons, electrons and positrons. The neutrino diffusion outward (towards the neutrinosphere) is then driven by the temperature gradient. The neutrinosphere is determined by the condition that optical thickness of the layer above it, for electron neutrinos with mean energy corresponding to T at the neutrinosphere, be unity.

The effect of high s on the EOS of the shocked envelope of a PNS can be seen by comparing the pressure-mass density dependence in the low and high entropy cases (Fig. 1). For $s = 5$ the pressure increases by more than an order of magnitude at $\rho = 10^{13}$ g cm^{-3}, as compared to the case with $s = 1$; the relative effect of s on p decreases with decreasing density. Above 10^{12} g cm^{-3}, the effect of trapped lepton number on the EOS of shocked envelope with $s = 5$ is much smaller than that of s.

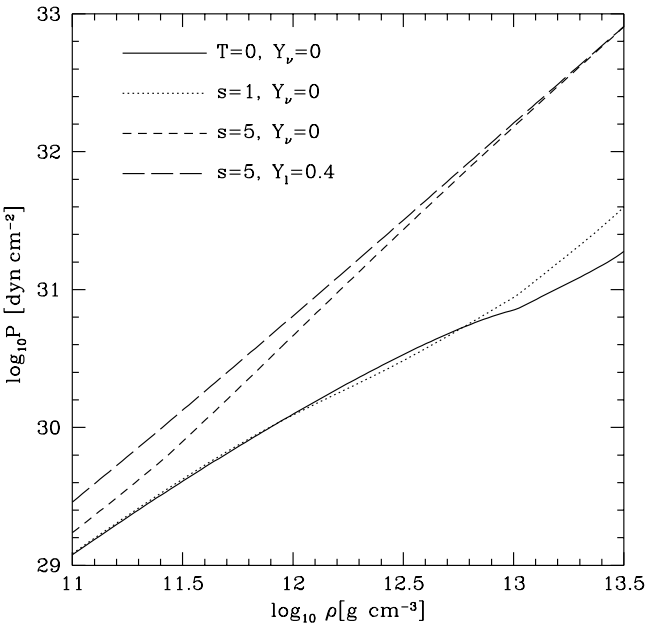

Fig. 1. Pressure versus matter density in the shocked ($s = 5$) envelope of a PNS (dashed and long-dashed lines). Two curves correspond to two limiting cases of trapped lepton number: long dashes - maximal trapped lepton fraction $Y_l = 0.4$; short dashes - no trapped lepton fraction ($Y_\nu = 0$). For the sake of comparison, we show also the EOS in the standard NS case of cold matter (solid line, $T = 0$), and that corresponding to low entropy and no trapped lepton number (dotted line, $s = 1$, $Y_\nu = 0$).

Actually, our models of EPNS were constructed only with a $Y_\nu = 0$ shocked envelope. This was done mostly for the sake of simplicity, and also to counterbalance some oversimplifications of our model with constant trapped lepton fraction, which would clearly overestimate the role of neutrinos (in numerical simulations, Y_l decreases outward, c.f., Keil et al. 1996). However, we think that a more detailed treatment of the shocked envelope would not change our main conclusions. On one hand, the layer with $\rho < 10^{12}$ g cm^{-3}, in which the assumption of $Y_\nu = 0$ could lead to a significant underestimating of pressure (Fig. 1), contains a very small fraction of the stellar mass. On the other hand, the inclusion of $Y_\nu > 0$ would further stiffen the EOS of the shocked envelope, and could only make our conclusions concerning the role of the shocked envelope even stronger (see Sect. 5.1).

2.2. Timescales and stationarity

The EOS of PNS evolves with time, due to the deleptonization, which changes the composition of the matter, and due to temperature change. However, significant changes of both T and Y_l within the hot, neutrino opaque interior occur on a timescale of seconds, if only diffusive processes are operating. The evolutionary timescales can be shortened, if convective transport is included. Still, these evolutionary timescales are orders of magnitude longer than the dynamical timescale, governing the readjustment of pressure and gravity forces.

Our treatment of PNS is based on the assumption, that convective motions do not influence directly the bulk mechanical equilibrium of rotating PNS. For the convective motions to be not important dynamically, convective matter velocities should be significantly smaller than the sound velocity within the neutrino opaque PNS interior. Velocity of sound, $v_{\rm s}$, can be calculated from the EOS of the PNS matter using

$$\left(\frac{v_{\rm s}}{c}\right)^2 = \gamma \frac{p}{e+p} \ , \qquad (1)$$

where e is the mass-energy density, and the adiabatic index γ is defined by

$$\gamma = \frac{n}{p}\left(\frac{{\rm d}p}{{\rm d}n}\right)_{Y_l,s} \ . \qquad (2)$$

In the case of cold NS matter the appropriate γ is that calculated at a fixed Y_e (Gondek et al. 1997).

In Fig.2a we plot the values of $v_{\rm s}/c$ versus matter density, within the shocked envelope of a PNS, and compare these values with those corresponding to different physical conditions in this density interval. The sound velocity in the shocked envelope ($s = 5$) is significantly higher than that corresponding to the matter at $s = 1$. Strongest effect of high s is seen for $\rho > 10^{12}$ g cm^{-3}. Trapped lepton number increases $v_{\rm s}$, but its effect is relatively small as compared to that of $s = 5$ for $\rho > 10^{12}$ g cm^{-3}. Sound velocity in the shocked envelope is significantly higher than the velocities of convective motions at the early stage of evolution of a protoneutron star obtained in numerical calculations (Keil et al. 1996). This conclusion is even stronger in the case of the unshocked core (Fig. 2b). The effect of finite entropy on the value of $v_{\rm s}$ is there negligible, because of the strong degeneracy of the matter, while trapped lepton number slightly decreases it.

A very important timescale is that of viscous dissipation of differential rotation. In the absence of convection and turbulence, shear viscosity is due to the diffusion of neutrinos. We will estimate the neutrino viscosity under the conditions prevailing in the dense hot core of PNS, using the general scheme of van den Horn & van Weert (1981a,b, 1984) for the calculation of transport coefficients of neutrinos trapped in dense, hot matter, combined with

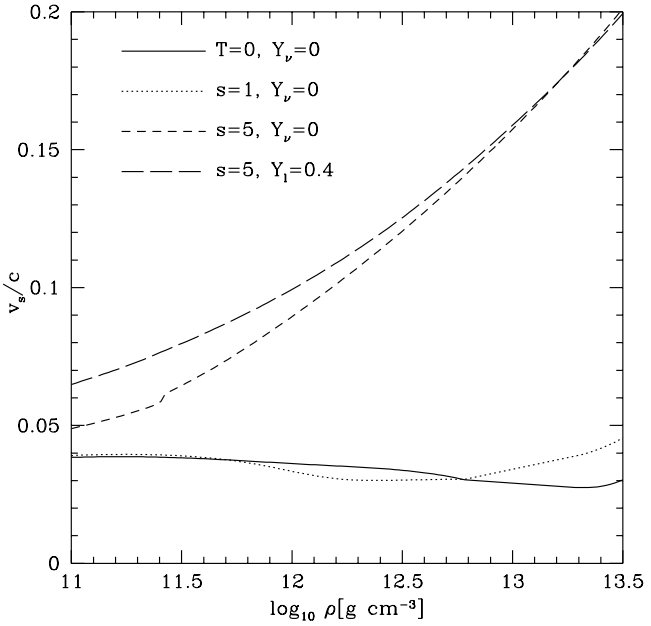

Fig. 2. a. Velocity of sound (in the units of the velocity of light c) versus matter density, in the bloated envelope of PNS (dashed line and long-dashed line). The density is bounded from above by that corresponding to our assumed value of $n_{\rm env}$. The case of $Y_\nu = 0$ (short dashed line) corresponds to no trapped lepton number, while that of $Y_l = 0.4$ (long-dashed line) is that of maximum trapped lepton number. For the sake of comparison, we show also the case of cold matter (solid line, $T = 0$), and that with low entropy and no trapped lepton number (dotted line, $s = 1$, $Y_\nu = 0$).

neutrino mean free paths as quoted in Burrows & Lattimer (1986). We obtain three expressions, corresponding to three different physical regimes for dense hot matter with trapped neutrinos. The earliest epoch corresponds to strongly degenerate electron neutrinos. In the dense PNS core, nucleons are degenerate, and neutrino viscosity in this regime (referred to as ${\rm D}n, {\rm D}\nu$), resulting from transport of degenerate electron neutrinos, is

$$\eta_\nu({\rm D}n, {\rm D}\nu) \ \simeq \ 3.1 \cdot 10^{23} \ \rho_{14} \times \\ \times (Y_\nu/0.05)(T/10 \ {\rm MeV})^{-2} \ {\rm g \ cm^{-1} \ s^{-1}}, \qquad (3)$$

where $\rho_{14} = \rho/(10^{14}$ g cm$^{-3})$ (our formula is in good agreement with the results obtained by Goodwin & Pethick (1982), who used the methods of the theory of Fermi liquids). After deleptonization, neutrinos become non-degenerate, and the neutrino viscosity in degenerate nucleon gas becomes somewhat lower,

$$\eta_\nu({\rm D}n, {\rm ND}\nu) \ \simeq \ 9.7 \cdot 10^{22} \times \\ \times (T/10 \ {\rm MeV})/\rho_{14}^{2/3} \ {\rm g \ cm^{-1} \ s^{-1}}. \qquad (4)$$

Finally, at subnuclear densities we can have non-degenerate neutrinos trapped in a dense hot nucleon gas, which

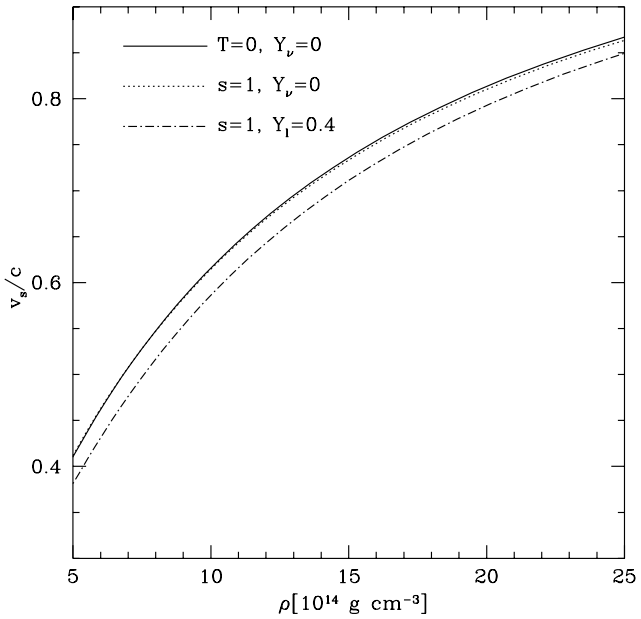

Fig. 2. b. Velocity of sound (in the units of velocity of light c) versus matter density, within the protoneutron star core ($n > n_{\rm core}$). Notation as in Fig. 2a.

corresponds to

$$\eta_\nu(\mathrm{ND}n, \mathrm{ND}\nu) \simeq 2.3 \cdot 10^{23} \times \times (T/10\ \mathrm{MeV})^2/\rho_{13}\ \mathrm{g\ cm^{-1}\ s^{-1}}. \quad (5)$$

In all cases the viscous timescales within the stellar interior, $\tau_\nu = l^2\rho/\eta_\nu$, with $l \sim 10$ km, are much longer than the lifetime of a PNS. Both magnetic field effects and local turbulence could shorten viscous timescales, but they are expected to be still much longer than the dynamical timescale.

The above discussion shows, that evolutionary timescales within a PNS, resulting from the transport processes in the stellar interior, are significantly longer than the dynamical timescale for PNS. In view of this, we are able to decouple the PNS evolution from its dynamics. We can then treat PNS rotation in a stationary approximation, with a well defined EOS of the PNS matter.

3. Formulation of the problem

The problem of the calculation of the stationary state of differentially rotating cold neutron stars, within the framework of general relativity, was considered previously by some authors (Komatsu et al. 1989, Wilson 1972, 1973), who restricted themselves, however, to polytropic (and hence unrealistic) EOS of dense matter. Here we will extend the methods used at $T = 0$ to the case of hot PNS with realistic EOS. We will use the notation and formalism developed in Bonazzola et al. (1993), hereafter referred to as BGSM.

3.1. Equation of stationary motion

As we already mentioned in paper I, one of the problems introduced by finite temperature and differential rotation, if one does not make any further assumption on the equilibrium configuration, is that the equation of stationary motion does not have a first integral (Bardeen 1972). This equation reads (eq. (5.8) of BGSM) :

$$\frac{\partial_i p}{e+p} + \partial_i \ln(\frac{N}{\Gamma}) = -F\partial_i\Omega\ , \quad (6)$$

where p is the pressure, e the mass-energy density, N the lapse function appearing in the space-time metric, Γ is the Lorentz factor due to rotation, Ω is the angular velocity and $F = u_\phi u^t$ where u is the fluid 4-velocity.

This equation is the general relativistic equivalent of a well-known Newtonian formula (see e.g. Tassoul 1978). It is straightforward to show that a *sufficient* condition for (6) to be integrable is

$$T = T(n)\ . \quad (7)$$

Eq.(6) can then be rewritten

$$\partial_i[G + \ln(\frac{N}{\Gamma})] = -F\partial_i\Omega\ , \quad (8)$$

where the heat function G is defined by

$$G = \int \frac{dp}{e(n,T(n)) + p(n,T(n))}\ , \quad (9)$$

which is not to be confused in non-isentropic cases with the logarithm of the dimensionless relativistic enthalpy per baryon $H = \ln(f) = \ln[(e+p)/(nm_0c^2)]$ (see paper I). Then, as in BGSM (§5.1), we apply the Schwarz theorem and find that either

$$\Omega = const. \quad (10)$$

or

$$F = F(\Omega). \quad (11)$$

This corresponds to the well-known result that, assuming barotropic equilibrium ($T = T(n)$), the rotation of the star is either uniform or cylindrical. Being interested in differential rotation, we restrict ourselves to the case (11).

The rotation law is obtained by solving Eq. (5.17) of BGSM (we correct here a misprint of this paper) :

$$F(\Omega) - \frac{A^4B^2r^2\sin^2\theta(\Omega - N^\phi)}{N^2 - A^4B^2r^2\sin^2\theta(\Omega - N^\phi)^2} = 0, \quad (12)$$

where A, B are metric potentials and N^ϕ is the shift vector (see BGSM for a precise definition).

One then obtains the first integral of motion in the form :

$$G + \ln(\frac{N}{\Gamma}) + \int F(\Omega) d\Omega = const. \quad (13)$$

This enables us to calculate G in the whole star and thus the other thermodynamic quantities, using the G-tabulated EOS of the form $e = e(G)$, $p = p(G)$, $s = s(G)$ (see §4.2).

Finally, in the case of general relativistic thermal equilibrium, one can show, in the context of the Eckart (1940) or Carter (1983) theory of heat diffusion, that

$$T^\star = T\frac{N}{\Gamma} e^{\int F d\Omega} = const. \quad (14)$$

where $T^\star$ is the redshifted temperature which would be measured by a distant observer, corresponds to thermal equilibrium (no heat flux). Such a T-profile leads to a simple form for the first integral of motion :

$$\mu^\star = \mu\frac{N}{\Gamma} e^{\int F d\Omega} = const. \quad (15)$$

where μ is the baryon chemical potential. The T-profile is then determined from

$$\frac{\mu(n, T(n))}{T(n)} = const. \quad (16)$$

which allows us to use the previous formulation (13) of the first integral of motion.

3.2. Differential rotation law

There is obviously an infinite number of degrees of freedom in the choice of the F-law. However, we wish to have a law which: (1) approximately reproduces the Ω-profile obtained in 2D-simulations, i.e. essentially decreases toward the edge of the star; (2) is a "simple" law, in order to limit the number of free parameters. We thus chose the rotation law used by Komatsu et al. (1989) :

$$F(\Omega) = R_0^2(\Omega_c - \Omega) \quad (17)$$

where Ω_c is the central angular velocity and R_0^2 is a free parameter, with the dimension of the square of a length (denoted A in Komatsu et al. 1989). This simple rotation law allows for a rapid solution of (12) since it becomes then a cubic equation.

In the Newtonian limit, the rotation law (17) yields the angular velocity

$$\Omega = \frac{R_0^2\Omega_c}{R_0^2 + r^2\sin^2\theta}. \quad (18)$$

We see that R_0 is thus a characteristic scale of spatial variation of Ω : when R_0 is small the rotation profile is very steep, leading to a constant specific angular momentum distribution, and when it is large the rotation is almost uniform. Numerical experiments have shown that the general relativistic profile has the same qualitative properties as the Newtonian one. Note that this Newtonian profile is also the equivalent, for cylindrical rotation, to the one used by Mönchmeyer & Müller (1989) and Janka & Mönchmeyer (1989) at the beginning of their calculations with spherical rotation. It is also the one used by Müller and Eriguchi (1985) in their calculations of "fizzling" white dwarfs.

3.3. Stability of differentially rotating PNS

Differentially rotating self-gravitating bodies are subject to various dynamical instabilities, which may deeply affect their structure (see e.g. Zahn 1993). In what follows, we study to what extent our models of hot PNS are stable regarding the two main axisymmetric instabilities due to the differential character of rotation, appearing in barotropic configurations : the Rayleigh and the shear instability. We then briefly discuss the case of secular instabilities linked to the spontaneous symmetry breaking phenomenon.

3.3.1. Rayleigh instability

It is straightforward to show that the newtonian Ω-profile (18) satisfies the classical Rayleigh stability criterion, i.e. :

$$\frac{\mathrm{d}j}{\mathrm{d}(r\sin\theta)} = \frac{\mathrm{d}(r^2\sin^2\theta\Omega)}{\mathrm{d}(r\sin\theta)} > 0, \quad (19)$$

where j is the specific angular momentum of baryonic matter. This criterion yields also a *sufficient* condition for stability in the case of cylindrical rotation laws, i.e.

$$\frac{\mathrm{d}j}{\mathrm{d}\Omega} < 0, \quad (20)$$

and one can show that the general relativistic Ω-profile obtained with the law (17) fulfils this last condition *in the isentropic case* (Komatsu et al., 1989, §3.1). For the full general relativistic formulation in non-isentropic cases, we checked that all our models verified (19). As this stability analysis is a local one in which the gravity does not enter, we infer that (19) is a good criterion even in the general relativistic case.

3.3.2. Shear instability

The case of the shear instability is much more complicated, and we will restrict ourselves to crude estimates. Our configurations, in which the Reynolds number (which compares turbulent to molecular viscosity) is of the order of $Re = R^2\rho\Omega/\eta \sim 10^3$ (see Section 2.2), are very likely to be unstable (see Zahn 1993). In principle, this instability could be blocked by a stable entropy or specific angular

momentum stratification inside the star. However, even if the entropy and specific angular momentum gradients of our models were all stable (apart from a thin outer layer of the star), these gradients are too weak to stabilize the flow. Indeed, the Richardson number Ri, which compares the efficiency of the stabilizing s and j-gradients to destabilizing effect of shear, can be written in the Newtonian case as

$$Ri = \left[\left(g - \frac{j^2}{r^3}\right)\left(\frac{1}{\gamma}\frac{\mathrm{d}\ln(p)}{\mathrm{d}r} - \frac{\mathrm{d}\ln(\rho)}{\mathrm{d}r}\right) + \frac{1}{r^3}\frac{\mathrm{d}j^2}{\mathrm{d}r}\right] \times \times \left(\frac{\mathrm{d}U}{\mathrm{d}r}\right)^{-2} \quad (21)$$

where g is the gravitational acceleration, γ the adiabatic index, ρ the mass density and $\mathrm{d}U/\mathrm{d}r$ the vorticity. In view of the fact, that our models are almost adiabatic, i.e. that

$$\left| \frac{1}{\gamma}\frac{\mathrm{d}\ln(p)}{\mathrm{d}r} - \frac{\mathrm{d}\ln(\rho)}{\mathrm{d}r} \right| < 0.5 \quad (22)$$

in the whole star, and that as R_0^2 decreases the j-distribution tends to a $j = const.$ one (giving thus a marginally Rayleigh-stable stratification), it was not a surprise to find that almost all our models verified $Ri < Ri_{\mathrm{crit}} = \frac{1}{4}$ (at least in some part of the star), which is a sufficient condition for instability.

However, the global effect of the shear instability is to suppress the phenomenon that causes it, namely, differential rotation. As the maximum angular momentum of PNS decreases with decreasing differential rotation (see §5), the introduction of this instability can only decrease the maximum angular velocity of such stars.

3.4. Non-axisymmetric instabilities

A rapidly rotating PNS can be affected by secular instabilities, driven by the gravitational radiation reaction (GRR instability) or by viscous dissipation. However, detailed calculations performed for hot uniformly rotating NS suggest that, for temperatures exceeding 10^{10}K, the GRR instability can only slightly decrease the maximum rotation frequency (Cutler et al. 1990, Ipser & Lindblom 1991, Lindblom 1995, Yoshida & Eriguchi 1995, Zdunik 1996). If the instability is driven by viscous dissipation, Bonazzola et al. (1995) have shown for cold uniformly rotating NS that only very stiff equations of state are likely to allow for spontaneous symmetry breaking.

As our models are differentially rotating and hot, no previous study applies to our EPNS and LPNS. To estimate to what extent our models could be plagued by spontaneous symmetry breaking, we used the *newtonian* criterion of stability $T/|W| < 0.14$, where T is the kinetic energy and W the gravitational energy of the star. As our PNS models are slowly rotating compared to cold NS, we were not surprised to find that $T/|W| \ll 0.14$ for the EPNS models. For LPNS, we found some models for which $T/|W| \sim 0.12-0.14$, which, considering the approximate criterion we used, cannot be viewed as conclusive of symmetry breaking. Furthermore, inclusion of symmetry breaking effects can only decrease the maximum angular momentum of PNS and thus, their maximal rotational velocity, which would only strengthen our conclusions.

4. Numerical method

4.1. Axisymmetric code

We used the same code based on spectral methods as in paper I, modified to take into account differential rotation. We refer the reader to our previous paper for a brief description of the code and tests of precision, which we made in the case of uniform rotation. Here we briefly outline the different or new features of the code.

The global relative error, evaluated by the means of the virial identity test (see BGSM), is $\sim 10^{-5}$. This is by two orders of magnitude better than the precision reached in paper I. Such an increase of precision was possible due to new interpolation procedure used for the EOS (see next section).

We used two grids in r for the star and one in the $1/r$-variable for the exterior, of N_r Chebychev coefficients, with $N_r = 65$ in the interior and $N_r = 33$ in the exterior, and one grid in θ with $N_\theta = 33$. We checked that taking a greater N_r or N_θ does not change the results by more than a few 10^{-6} at most, which stays within the global precision reached. Let us stress that such a low number of grid points is sufficient to reach high accuracy within a spectral method (this would not be possible in the case of a finite difference scheme).

The temperature drop at the "neutrinosphere" is not always located on the border of the internal grid in r, which could influence the precision (remember that the spectral methods are very sensitive to discontinuities). We checked that, in fact, even when the "neutrinosphere" is far from the border of the grid, the global physical properties of the star did not change much for the late-type models of PNS (we found also relative variations of a few 10^{-6} at most). For early-type models of PNS, the results were more sensitive to the location of the "neutrinosphere", and we were obliged to position the grids quite precisely to reach the former precision.

4.2. Interpolation procedure for the EOS

The precision of the axisymmetric code is very sensitive to the thermodynamic consistency of the interpolated EOS. In particular, the following thermodynamical relation must be fulfilled to ensure a good precision of the code,

$$\frac{\mathrm{d}p}{\mathrm{d}G} = e + p \; . \quad (23)$$

If the above relation is only approximately fulfilled by the EOS (as is the case when various thermodynamical quantities are independently interpolated) the equation of stationary motion cannot be strictly satisfied, neither. This influences greatly the value of the virial parameter and thus, the precision of the calculations. In order to have a consistent EOS (in the sense that (23) is verified), we used an original procedure, adapted from a method derived by Swesty (1996).

Once the temperature profile is chosen, the EOS can be tabulated. The heat function G is calculated by interpolating the quantity $1/(e+p)$ in the integrand in Eq.(4) as a function of p using cubic splines and integrating this interpolating polynomial. The quantity G can then be chosen as the new interpolation variable : as this is a quantity given directly by the first integral of motion (see §3) this ensures a rapid calculation of the thermodynamical quantities. Futhermore, following Swesty, we use the fact that $\mathrm{d}p/\mathrm{d}G$ is known and interpolate p and $\mathrm{d}p/\mathrm{d}G$ by means of a Hermite interpolation scheme of degree 3. The energy density is obtained at each point by derivating the interpolant and using (23). Other thermodynamical quantities can be interpolated independently since they do not enter this relation. In doing so, we ensure that (23) is valid for the whole interpolation polynomial and not only at the interpolation points.

With such an interpolation procedure, we were able to lower the virial error parameter by two orders of magnitude.

5. Numerical results

5.1. Static models of early-type PNS and "minimal mass" limit

Early-type PNS, with a high-entropy, bloated envelope, are short living structures. Their lifetime might be as short as 100-200 ms (if one includes convective motions, see Keil et al. 1996), but this is still a long time on a dynamical timescale. As early-type models of PNS have not been investigated in paper I, we study here the static properties of these objets. The gravitational and baryonic mass of static models versus central baryonic density are displayed in Fig. 3. Let us notice, that we have restricted ourselves to the range of masses, consistent with assumed thermal structure of PNS. As one can see, there is a minimal mass for such equilibria, as for cold ones, but it is of the order of $M_{\rm bar}^{\rm min}(\mathrm{EPNS}) \sim 1.4\ \mathrm{M}_\odot$, much higher than the standard minimal mass of cold NS ($M_{\rm bar}^{\rm min}(\mathrm{NS}) \sim 0.1\ \mathrm{M}_\odot$). This high minimal mass of EPNS is due to the fact that thermal pressure at the base of the neutrinosphere tends to blow-off the envelope of the star, and thus additional mass compared to the cold case is needed to preserve equilibrium. This effect was already present in the models of paper I, but we were at that time interested in the maximal mass of PNS and did not investigate this problem.

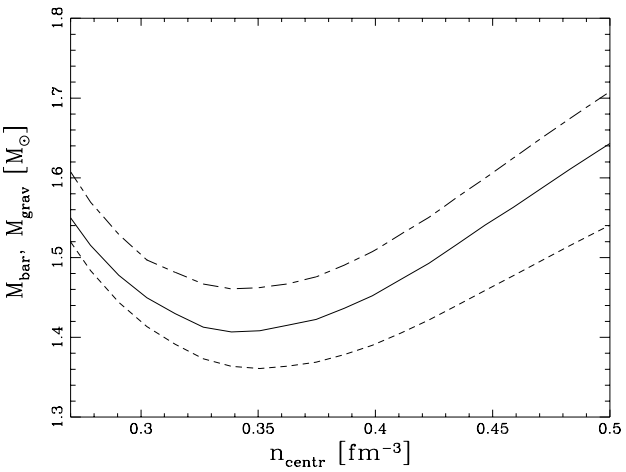

Fig. 3. Baryon and gravitational mass of static models of early-type PNS versus central density, $n_{\rm centr}$. The solid curve is for baryonic mass and the dashed curve for gravitational mass. The upper long-dash/short-dash curve is the baryon mass, $M_{\rm bar}$, calculated for differentially rotating configurations at $R_0^2 = 1\ \mathrm{km}^2$ and $R\Omega_c = 0.284$ c, where R is the star radius. This illustrates the effect of rotation on the minimal baryonic mass. The parameters of the EOS chosen are $s_{\rm env} = 5$, $s_{\rm core} = 1\ \mathrm{k_B}$, $n_{\rm env} = 0.02\ \mathrm{fm}^{-3}$ and $n_{\rm core} = 0.26\ \mathrm{fm}^{-3}$, with $Y_l = 0.4$ in the core and $Y_\nu = 0$ in the shocked envelope.

For late-type PNS, the minimal mass is increased at most up to $M_{\rm bar}^{\rm min}(\mathrm{LPNS}) \sim 0.9\ \mathrm{M}_\odot$ (Gondek et al., 1997).

The value of $M_{\rm bar}^{\rm min}(\mathrm{EPNS})$ is strongly linked to the properties of our EOS, through the assumed values of the EOS parameters. Table 1 displays the minimal masses reachable for various combinations of the parameters of the EOS.

For some sets of parameters, minimal baryonic mass is larger than $1.5\ \mathrm{M}_\odot$. In particular, we found that for $s_{\rm env} \geq 6$, the minimal baryonic mass is greater than $1.5\ \mathrm{M}_\odot$ and therefore no static equilibrium can be found for our "canonical" baryon mass. Let us notice, that the value of minimal mass is not sensitive to the presence of trapped neutrinos in the unshocked core : had we taken a neutrino free core, the minimal mass would change only by a few percent as compared to that calculated assuming $Y_l = 0.4$.

Let us stress, that EPNS models with $n_{\rm centr}$ lower than that corresponding to the minimum mass configuration (i.e., those to the left of the minima of the mass - central baryon density curves in Fig. 3) are rather unrealistic, and moreover likely to be unstable. They consist mostly of the shocked, high entropy matter. Clearly, such objects could not be formed in a successful SN II explosion: too much of the shock energy would be dissipated for heating and dissociating the collapsing matter.

The very existence of a high minimal baryonic mass for static configurations of early-type PNS leads to severe constraints on their rotational velocity or, more precisely,

Table 1. Minimal baryonic masses of EPNS for various values of the parameters of the EOS.

$s_{\rm env}$	5	4	5	5	5	5
$s_{\rm core}$	1	1	2	1	1	1
$n_{\rm env}$ [fm^{-3}]	0.02	0.02	0.02	0.02	0.02	0.01
$n_{\rm core}$[fm^{-3}]	0.26	0.26	0.26	0.3	0.1	0.26
$M_{\rm bar,min}$ [M$_\odot$]	1.41	1.23	1.56	1.50	1.19	1.22

on the maximal angular momentum they can bear. As one increases the central angular velocity of such stars, keeping their baryonic mass constant, the centrifugal force adds to the thermal pressure at the base of the envelope. The envelope is then more easily lifted than in the static case, leading to an increase of the minimal mass of stationary configurations. At the "minimal mass" limit, the minimal mass coincides with the canonical one and no equilibrium can be found with a higher angular momentum. So, apart from the usual keplerian - or "mass shedding" - limit (for which the centrifugal force exactly balances the gravity at the equator), this "minimal mass" limit also constrains the domains of variations of Ω_c and R_0^2.

5.2. Variations of J versus Ω_c for early-type PNS

Given the two limits constraining Ω_c and R_0^2, the problem remains of finding the maximal angular momentum of EPNS. Variations of the angular momentum versus central rotational velocity were previously studied for cold uniformly rotating NS with various realistic EOS (Cook et al. 1992, 1994, Salgado et al. 1994). These studies showed that there exist two distinct families of uniformly rotating cold NS : *normal* and *supra-massive* stars. Normal stars have a baryonic mass lower than the maximal static baryonic mass, and their angular momentum is an increasing function of the central angular velocity. Supra-massive stars have baryonic mass greater than the maximal static baryonic mass, which they would thus not support without rotation. Their angular momentum is not a monotonic function of the central angular velocity, and the stable keplerian configuration is not that of maximal angular momentum. This property leads so to the well-known phenomenon of "spin-up by angular momentum loss".

As the canonical mass we chose ($M_{\rm bar} = 1.5$ M$_\odot$) is less than the maximal static baryonic mass for all the EOS we used, we expected that, for a given Ω-contrast (a given R_0^2), J would increase with increasing central angular velocity for our models of PNS. Numerical experiments showed that this is indeed the case for cold models but *not* for the hot ones. This can be understood as follows. For cold uniformly rotating NS, the phenomenon of spin-up by angular momentum loss is due to the high oblateness of the supra-massive stars due to their high rotational velocities

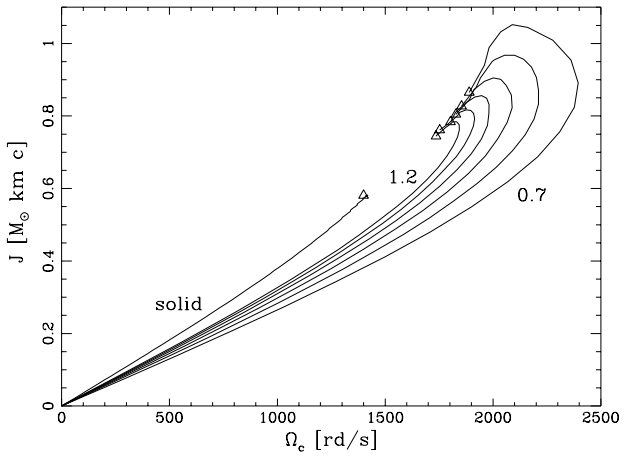

Fig. 4. a. Angular momentum versus central angular velocity of EPNS of baryon mass 1.5 M$_\odot$, for rigid rotation and for differential rotation with R_0^2 = 1.2, 1.1, 1.0, 0.9, 0.8 and 0.7 km^2 (from the left to the right). The parameters of the EOS are as in Fig. 3. Triangles denote the keplerian configurations.

(see Cook et al., 1992, 1994) : since $\Omega = J/I$, the variations of Ω depend on the variations of both J and I, for a sufficiently extended star, the redistribution of I when one increases Ω can lead to a decreasing J. This effect is thus strongly linked to the radial distribution of matter inside the star, and can be significantly enhanced by the presence of differential rotation (Shapiro et al., 1990), but nevertheless appears *only* in supra-massives stars. This is not the case for PNS. Due to their extended structure induced by the supplementary thermal pressure, very little rotation is needed to produce this phenomenon. Thus it can appear even in *normal* PNS.

Figures 4a and 4b depict typical behaviours of J as a function of Ω_c : starting from the static model, we increase the quantity $R\Omega_c$ (which parametrizes our models) up to the limiting configurations, keeping the baryonic mass and R_0^2 constant. As one can see, the "spin-up" phenomenon is not present for uniformly rotating shocked PNS. Differential rotation has the effect of increasing the maximal central angular velocity and the maximal angular momen-

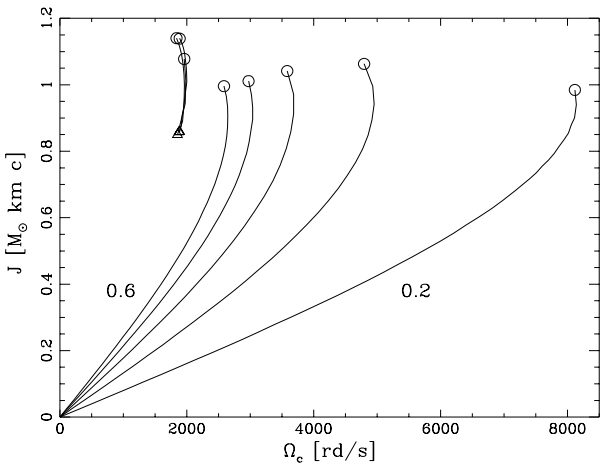

Fig. 4. b. Angular momentum versus central angular velocity of early-type PNS, of baryon mass 1.5 $M_\odot$, for differential rotation with R_0^2 = 0.6, 0.5, 0.4, 0.3 and 0.2 km^2 (from the left to the right). The parameters of the EOS are as in Fig. 3. Triangles denote the keplerian configurations and circles are for configurations with $M_{\rm bar}^{\rm min} = 1.5$ $M_\odot$ ("minimal mass" limit configurations). The upper-left curves are the $J_{\rm ms} < J < J_{\rm mm}$ parts of the $R_0^2 = 0.6$, 0.5, 0.4 km^2 curves (see text).

tum $J^{\rm max}$, "pushing" the curves to the right and the top in Fig. 4. It also increases the angular momentum $J_{\rm ms}$ at which mass shedding appears (configurations denoted by triangles on Fig. 4a) : $J_{\rm ms}$ is an increasing function of $1/R_0^2$.

The two physical limits previously mentioned restrain the available maximal angular momentum. For small Ω-contrast (large R_0^2), the mass shedding limit is reached first, and one cannot store enough angular momentum in the star to reach the "minimal mass" limit at $J = J_{\rm mm}$: this is the case for all the configurations of Fig. 4a, for which the angular momentum J verifies $0 \leq J < J^{\rm max}$, with $J_{\rm ms} < J^{\rm max} < J_{\rm mm}$. Let us stress that in the case of cold uniformly rotating normal NS, one has always $J^{\rm max} = J_{\rm ms}$ for a fixed $M_{\rm bar}$, which is never the case for the differentially rotating sequences displayed in Fig. 4a, b.

As we decrease R_0^2, $J^{\rm max}$ increases and the $J^{\rm max}$ configuration will finally reach the minimal mass limit for $J^{\rm max} = J_{\rm mm} \sim 1$ $M_\odot$ km c for the EOS we chose. With a further increase of the Ω-contrast (decrease of R_0^2), the $J - \Omega_{\rm c}$ plot at fixed $M_{\rm bar}$ divides into two disconnected segments (branches). The first branch, which starts at $\Omega_{\rm c} = 0$, ends at the minimum mass limit with $J_{\rm mm}$. A second segment (upper left curves in Fig. 4b) is bounded from above by another minimum mass limit, $J'_{\rm mm}$ (which is actually an overall maximum of J for a specific value of R_0^2), and from below by the mass shedding limit with $J_{\rm ms}$. Notice, that these segments evolved from the upper left parts of the J–$\Omega_{\rm c}$ curves in Fig. 4a, with the very upper part removed by the minimum mass constraint. The upper left segments correspond to rotating configurations with $J_{\rm ms} \leq J \leq J'_{\rm mm} = J^{\rm max}$. Such a situation is characteristic of a rather narrow range of the R_0^2 parameter (R_0^2 = 0.6, 0.5 and 0.4 km^2 in Fig. 4b). For a still larger Ω-contrast (still smaller R_0^2) the left segment disappears and we are left only with the configurations verifying $0 \leq J \leq J_{\rm mm} = J^{\rm max}$ (curves with R_0^2 = 0.3, 0.2 km^2 in Fig. 4b).

We show in Fig. 5a and 5b the constant energy density lines in the cross sections of two typical limiting configurations of EPNS. As one can see, the keplerian configuration is a very extended one, with a "disk-like" shape due to the combined effect of differential rotation and of a high entropy envelope. The minimal mass limit configuration is more compact, with a "toroidal" shape. In both cases, small irregularities in the outermost (low density) constant energy density lines are due to the Gibbs phenomenon in the θ direction, a problem inherent in our numerical scheme but small enough not to affect badly the virial parameter (see sect. 4.1).

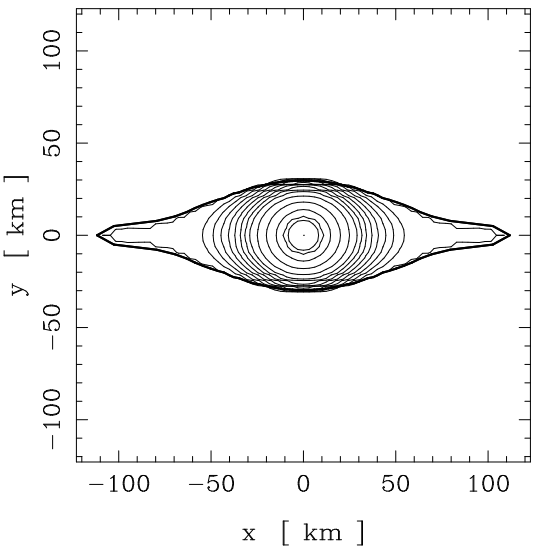

Fig. 5. a. Iso-energy density lines of the keplerian configuration of $M_{\rm bar} = 1.5$ $M_\odot$, with $R_0^2 = 0.5$ km^2 (corresponding to the triangle of the $R_0^2 = 0.5$ curve in figure 4b). x and y are related to the MSQI coordinates r and θ by $x = r\cos\theta$, $y = r\sin\theta$ (see BGSM for details).

5.3. Thermal structure and maximal angular momentum of PNS

Uniformly rotating models of late-type PNS, considered in Paper I, assumed a relatively homogeneous distribution of entropy within the neutrino opaque interior. In order to answer the question, to what extent the conclusions of Paper I would be modified by allowing for dif-

Table 2. Parameter $R_{0,\mathrm{crit}}$ for different states of the LPNS interior

EOS	$s_{\mathrm{core}}=2$ $Y_l=0.4$	$s_{\mathrm{core}}=1$ $Y_l=0.4$	$T^\star=15$ MeV $Y_\nu=0$	$T^\star=25$ MeV $Y_\nu=0$
$R^2_{0,\mathrm{crit}}$ [km^2]	1.044	1.091	0.916	0.894

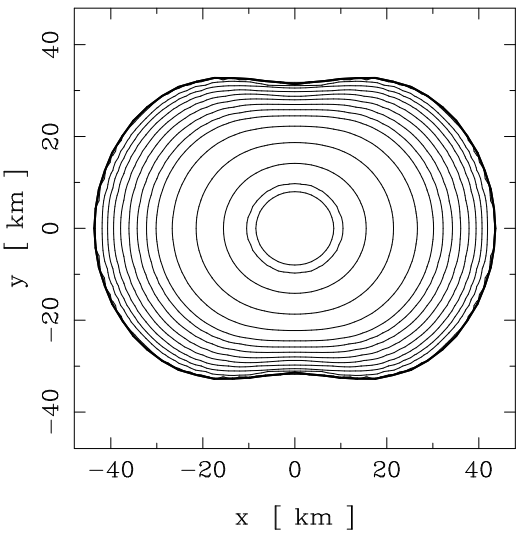

Fig. 5. b. Iso-energy density lines of the minimal mass limit configuration of $M_{\mathrm{bar}}=1.5$ M$_\odot$, with $R_0^2=0.5$ km^2 (corresponding to the upper right circle of the $R_0^2=0.5$ curve in figure 4b).

ferential rotation, we considered models, which were isentropic or isothermal within the neutrino opaque core. Let us mention, that such a homogeneous thermal state of a PNS corresponds to a relatively late switching-off of accretion due to the lift-off of the shock. Accretion stage had to be sufficiently long to allow for settling-down of the PNS envelope, and for the thermal uniformization of the neutrino-opaque interior. In what follows, we will restrict ourselves to the case of $M_{\mathrm{bar}}=1.5$ M$_\odot$. As in the case of two-component EPNS, described in the preceding section, we calculated $J(\Omega_c)$ sequences for fixed parameter R_0^2. We found, that there exist a specific value, $R_{0,\mathrm{crit}}$, such that for $R_0<R_{0,\mathrm{crit}}$ we get the maximum angular momentum of PNS which is larger than the maximum angular momentum of cold, uniformly rotating NS of the same M_{bar}. So, for $R_0<R_{0,\mathrm{crit}}$, differential rotation allows PNS to have enough angular momentum to yield cold NS, rotating uniformly at maximal angular velocity. The values of $R_{0,\mathrm{crit}}$ for the different EOS used in paper I are displayed in table 2. It should be stressed, that this qualitative conclusion is generally valid for thermally homogeneous LPNS, for all considered EOS of stellar interior (isentropic with $s\leq 2$, isothermal, with no trapped lepton number $Y_\nu=0$, and with maximum trapped lepton fraction $Y_l=0.4$), and that the actual value of $R_{0,\mathrm{crit}}$ is roughly independent of the assumed EOS.

For $R_0<R_{0,\mathrm{crit}}$, we can consider configurations having an angular momentum greater than the maximal angular momentum of cold NS. Such PNS will necessarily eject a part of J and M_{bar} during their evolution toward cold, uniformly rotating NS. This will probably lead to a maximally rotating (i.e., rotating at its mass shedding limit) NS surrounded by an ejected matter. For $R_0>R_{0,\mathrm{crit}}$, evolution of PNS into a cold NS leads to the final rotation frequency which is lower than the maximal one for such a cold NS, but the difference decreases with decreasing R_0.

Let us consider now the case of early-type PNS. Being aware of the particular behaviour of J depicted in the previous paragraph, we scanned the whole domain of $0.1<R_0^2<1$ km^2 for the maximal angular momentum of LPNS. In this domain, the maximal angular momentum configurations were never keplerian. We found that $1.0<J_{\max}<1.16$ M$_\odot$km c, which is roughly independent of R_0^2. As the crucial factor determining the "minimal mass limit" is the effective gravity at the base of the shocked envelope for large Ω-contrast, it is not surprising to find that our results are roughly *independent* of the parameter R_0^2 (thus, in some way, of the assumed rotation law), and depends *only* on the angular momentum of the star. These limits on the total angular momentum of the early-type PNS leads to limits on the period of cold NS of the same baryon mass of $1.6<P<1.8$ ms.

These results are relevant for NS which originate in a type II supernova and evolve *without significant accretion* from a hot, differentially rotating LPNS to a cold, uniformly rotating NS. If the baryonic mass of such a PNS is ~ 1.5 M$_\odot$, then the maximum frequency of the resulting NS cannot exceed ~ 600 Hz. This evolutionary argument thus imposes more stringent limits on the rotation rate of NS than standard calculations (Cook et al. 1994, Salgado et al. 1994).

6. Discussion and conclusions

In the present paper we studied models of rapidly differentially rotating protoneutron stars. Using realistic equations of state of the protoneutron star interior, we calculated, using general relativistic equations of stationary

motion, families of configurations corresponding to the main stages of evolution of protoneutron stars. The earliest stage corresponds to two-component objects, with a low entropy unshocked core and a bloated, high-entropy envelope. The next stage is that of a lepton rich protoneutron star, with a relatively uniform distribution of entropy per baryon within the hot neutrino-opaque core, containing degenerate neutrinos. Finally, the latest stage is that a deleptonized hot neutrino-opaque core, which contains non-degenerate neutrinos. We considered mostly the case of a protoneutron star of the "canonical baryon mass" 1.5 $M_\odot$, which roughly corresponds to measured gravitational masses of binary pulsars.

Configurations of stationary motion were calculated assuming axial symmetry, and neglecting effects of meridional circulation and convection. Such an approximation was valid, because the velocities of meridional circulation, as well as those connected with convective motion, were much smaller than the velocity of sound in the protoneutron star interior. On the other hand, they were also much smaller than the linear equatorial velocities considered. While convective motions could be assumed to have no direct dynamical effect, they influenced the PNS structure through changes in composition and temperature, through transport of heat and of lepton number, leading to the evolution of the equation of state of stellar interior. Our assumption that the local temperature was a function of local density was sufficient for the equations of stationary motion to be integrable; stationary state of differential rotation was then that of a barotropic equilibrium.

The approximation of stationarity was crucial for the simplicity of calculations. The shear viscosity, resulting from neutrino diffusion, implies angular momentum transport and heating of the stellar interior. However, the estimates of the characteristic timescales, under various regimes prevailing within the hot neutrino opaque core, imply that these effects can be neglected on the timescale of the PNS lifetime. Clearly, the timescale of angular momentum and energy transport can actually be significantly shortened by convective and turbulent motions within the stellar interior. Also, the presence of magnetic field, and subsequent amplifying of it due to the differential character of rotation (winding-up of magnetic field lines), could contribute to the angular momentum transport and to rigidifying of the rotational motion. However, even in this case characteristic timescales referring to the global structure of rotating star may be expected to be of the order of seconds. Clearly, all these effects which are expected to be operating in a differentially rotating protoneutron star, deserve a separate study.

Our models describe rotating PNS after revival and lift-off of the shock, i.e., after accretion onto PNS became insignificant for mechanical equilibrium. Basically, we considered two limiting scenarios of the 'liberation' of PNS from accretion. The first case corresponds to a relatively early switching-off of accretion, so that rotating PNS has still a pronounced two-component thermal structure, with an unshocked low entropy core and a shocked high entropy envelope. The second case is that of a relatively late lifting-off of the shock, when the accretion stage was sufficiently long to allow for mixing of the low and high entropy matter, leading to a roughly isentropic PNS interior. Let us notice, however, that the second scenario is, in view of very high accretion rate, quite risky for the PNS survival. Huge accretion rates (of the order of $M_\odot$/s) might result in a high probability of exceeding the maximum allowable mass for neutron stars, and therefore could easily lead to formation of a black hole.

For a "canonical baryon mass" of 1.5 $M_\odot$, and within the considered family of differentially rotating configurations, we find a set of configurations with angular momentum exceeding the maximum one that can be accommodated by rigidly rotating cold neutron stars of the same baryon mass. We expect, that the evolution of such differentially rotating protoneutron stars into cold, uniformly rotating neutron stars will be accompanied by ejection of matter from their equators. Such a mass shedding configuration may be expected to be susceptible to some additional instabilities, which - if breaking axial symmetry - could contribute to a further angular momentum loss via emission of gravitational radiation.

Assuming that the initial differentially rotating configuration had a characteristic two-component structure, with a high entropy envelope, containing some half of the baryon mass of the protoneutron star, we get (for a standard baryon mass of 1.5 $M_\odot$) a minimum period of resulting cold neutron star $P_{\rm min}^{\rm cold} \simeq 1.7$ ms. Shorter rotation periods of cold neutron star of the baryon mass of ~ 1.5 $M_\odot$ (such as the periods measured for the most rapid millisecond pulsars like PSR 0034-0534, PSR 1937+21, PSR 1957+20, see e.g. Bailes & Lorimer 1995) could then be reached only by a spin-up via accretion of a significant fraction of solar mass from an accretion disk.

Acknowledgements. We are very grateful to J-P. Zahn and S. Talon for introducing us to the difficult subject of instabilities in differentially rotating fluids. This research was partially supported by the JUMELAGE program "Astronomie France-Pologne" of CNRS/PAN and by the KBN grant No. P304 014 07. The numerical computations have been performed on Silicon Graphics workstations, purchased thanks to the support of the SPM department of the CNRS and the Institut National des Sciences de l'Univers.

References

Bailes M., Lorimer D., 1995, in "Millisecond Pulsars : A Decade of Surprise", ASP Conf. Ser., Vol. 78, Fruchter A.S., Tavani M. & Bacher D.C. eds.

Bardeen J.M., 1972, in "Black Holes - Les astres occlus", Les Houches, ed. De Witt C. & De Witt B.S., Gordon and Breach Sci. Pub., New York

Bombaci I., Prakash M., Prakash M., Ellis P.J., Lattimer J.M., Brown G.E., 1995, Nucl. Phys. A, 583, 623

Bombaci I., 1996, A&A 305, 871
Bonazzola S., Gourgoulhon E., Salgado M., Marck J.A., 1993, A&A 278, 421
Bonazzola, S., Frieben, J., Gourgoulhon, E., 1995, ApJ 460, 379
Burrows A., Lattimer J.M., 1986, ApJ, 307, 178
Burrows A., Hayes J., Fryxell B.A., 1995, ApJ, 450, 830
Carter B., 1983, in "A random walk in relativity and cosmology", Dadhich N., Krisna Rao J., Narlikar J.V. & Vishveshwara C.V. eds., Bombay
Cook G.B., Shapiro S.L., Teukolsky S.A., 1992, ApJ, 398, 203
Cook G.B., Shapiro S.L., Teukolsky S.A., 1994, ApJ, 424, 823
Cutler C., Lindblom L., Splinter R.J., 1990, ApJ 363, 603
Eckart C., 1940, Phys. Rev., 38, 919
Gondek D., Haensel P., Zdunik J.L., 1997, A&A 325, 217
Goodwin B.T., Pethick C.J., 1982, ApJ, 253, 816
Goussard J-O., Haensel P., Zdunik J.L., 1997, A&A 321, 822 (Paper I)
Hashimoto M-A, Oyamatsu K., Eriguchi Y., 1995, ApJ 436, 257
van den Horn L.J., van Weert C.G., 1981a, ApJ 251, L97
van den Horn L.J., van Weert C.G., 1981b, Phys. Lett. 83A, 88
van den Horn L.J., van Weert C.G., 1984, A&A 136, 74
Ipser J.R., Lindblom L., 1991, ApJ 373, 213
Janka H.T., Mönchmeyer R., 1989, A&A, 226, 69
Keil W., Janka H.T., Müller E., 1996, ApJ, 473, L111
Komatsu H., Eriguchi Y., Hachisu I., 1989, MNRAS 239, 153
Lattimer J.M., Swesty F.D, 1991, Nucl. Phys. A535, 331
Lindblom L., 1995, ApJ 438, 265
Mönchmeyer R., Müller E., in "Timing Neutron Stars", ed. Ögelman H. & van den Heuvel E.P.J., Kluwer Acad. Pub.
Müller E., Eriguchi Y., 1985, A&A, 152, 325
Prakash M., Bombaci I., Prakash M., Ellis P.J., Lattimer J.M., Knorren R., Phys. Reports, 280, 1
Salgado M., Bonazzola S., Gourgoulhon E., Haensel P., 1994, A&A, 291, 155
Sawyer R.F., Soni A., 1979, ApJ 230, 859
Shapiro S.L., Teukolsky S.A., Nakamura T., 1990, ApJ, 357, L17
Swesty F.D., 1996, J. of Comp. Phys., 127, 118
Takatsuka T., 1995, Nucl. Phys. A588, 365
Tassoul J.L., 1978, "Theory of rotating stars", Princeton University Press, Princeton
Wilson J.R., 1972, ApJ, 176, 195
Wilson J.R., 1973, Phys. Rev. Lett., 20, 1082
Yamada S., Sato K., 1994, ApJ, 434, 268
Yoshida S., Eriguchi Y., 1995, ApJ 438, 830
Zahn J-P., 1993, in "Astrophysical fluid dynamics", Les Houches, ed. Zahn J-P. & Zinn-Justin J., Elsevier Sci. Pub.
Zdunik, J.L., 1996, A&A 308, 828

This article was processed by the author using Springer-Verlag LaTeX A&A style file *L-AA* version 3.